Palladium Supported on Calcium Decorated Carbon Nanotube Hybrids for Chemoselective Hydrogenation of Cinnamaldehyde

Ying Ma[1,2†], Lu Feng[1,3†], Zhanglong Guo[1], Jiangtao Deng[1,3], Cuong Pham-Huu[4] and Yuefeng Liu[1]*

[1] Dalian National Laboratory for Clean Energy (DNL), Dalian Institute of Chemical Physics, Chinese Academy of Sciences, Dalian, China, [2] University of Chinese Academy of Sciences, Beijing, China, [3] Zhang Dayu School of Chemistry, Dalian University of Technology, Dalian, China, [4] Institute of Chemistry and Processes for Energy, Environment and Health (ICPEES), UMR 7515 CNRS-University of Strasbourg, Strasbourg, France

The chemoselective hydrogenation of cinnamaldehyde (CAL) to the corresponding hydrocinamaldehyde (HCAL) is a type of important reactions in fine chemistry, which is critically dependent on the rational design the chemical structure of active metal. In this work, calcium promoted palladium on CNT hybrid (Ca-Pd@CNT) with monolithic structure was synthesized through one-pot alginate gel process. The catalytic performance results showed that moderate Ca promotion catalyst (Ca-Pd@CNT$_{HCl-2h}$) present a superior CAL hydrogenation activity with CAL conversion of 99.9% and HCAL selectivity of 86.4% even at the lager Pd nanoparticle size (c.a. 5 nm). The characterization results show that the electron transfer between the additive Ca promoter and Pd nanoparticles (NPs) could modify the electron structure of Pd species and induce the formation of the partial positively charged Pd$^{\delta+}$ species on the Pd NPs surface in the Ca-Pd@CNT$_{HCl-2h}$ catalyst resulting to the satisfactory catalytic performance. Furthermore, the one-pot gel synthesis methodology for microscopic carbon supported catalyst could also endows its great potential industry application in heterogeneous catalysis with easily handling during the transportation and reaction, and attributed to reducing the overall pressure drop across in the fix-bed reactor.

Keywords: Pd nanoparticles, Ca promoter, electronic modification, cinnamaldehyde hydrogenation, monolithic nanocarbon materials

INTRODUCTION

Catalytically selective hydrogenation of α, β-unsaturated aldehydes via C=O or C=C bond to α, β-unsaturated alcohols or saturated aldehydes is considered as an important fine chemical process for producing intermediates for food additives and pharmaceuticals (Gallezot and Richard, 1998; Mäki-Arvela et al., 2005; Wu et al., 2012; Daly et al., 2014; Kahsar et al., 2014; Tian et al., 2015). However, the C=C and C=O bond are conjugated in the typical substrate of α, β-unsaturated aldehydes-cinnamaldehyde (CAL), which result in a mixture of hydrogenation products such as cinnamyl alcohol (COL), hydrocinnamaldehyde (HCAL), and 3-phenyl propanol (PPL). Palladium-based catalyst is favor to C=C hydrogenation due to its special position of d-band center. Therefore, Pd could work as the active metal center for hydrogenation of

CAL to produce the HCAL (Garcia-Mota et al., 2010; Ide et al., 2012; Cárdenas-Lizana et al., 2013; Arrigo et al., 2014; Salnikov et al., 2014; Durndell et al., 2015; Zhao et al., 2015). Tailoring the electronic structure of Pd active sites through adjustment surface chemistry of catalyst support (Balmes et al., 2012; Cárdenas-Lizana et al., 2013; Figueiredo, 2013; Arrigo et al., 2016; Rao et al., 2017), construction of the bimetallic or alloy composition (Vu et al., 2006; Tsang et al., 2008), regulation of the particle size (Amorim and Keane, 2008; Jiang et al., 2016; Xu et al., 2019) and the addiction of promoter (Tsang et al., 2008) could promote the CAL hydrogenation activity as well as the HCAL selectivity (Toebes, 2004; Jiang et al., 2016). The alkalis and alkaline-earth metals, such as Li, Na, K, Rb, and Sr, are reported as effective promoter cations for CAL hydrogenation (Galvagno et al., 1986; Li et al., 1997; Hsu et al., 2010; Bhogeswararao and Srinivas, 2012), which could increase the HCAL selectivity. Furthermore, alkalis and alkaline-earth metals as promoter could also modify the coordination environment around the noble metal atom through charge transfer between the active metal and the promoter, even forming new catalyst sites and thus regulating the catalytic properties (Song et al., 2006). Yang et al. (2017) found that the controlled addition of potassium with Pt/zeolite catalysts can create the Pt-O (OH)-K interfacial sites, which could greatly accelerated the reverse water gas shift reaction. Wei et al. (2017) also prepared Na cations modified the Pt/FeOₓ catalyst and the formed Pt-O-Na-O-Fe-like species could enhance the 3-aminostyrene selectivity significantly while the hydrogenation activity of 3-nitrostyrene remained unchanged. Considering the alkalis metal can act as the electronic modifiers, we proposed to regulate the activity and selectivity of cinnamaldehyde hydrogenation by controllable introducing Ca to modify the Pd-based catalyst and investigate the influence of calcium promoter. Meanwhile, the reaction rate could also be reduced due to the blocking or poisoning the active sites with inappropriate loading amount of Ca (Yang et al., 2017).

Compared to conventional metal oxides, carbon is an inert support, which can be used as a platform to disperse and study the changes of electronic state of metals (Auer et al., 1998; Su et al., 2013). Carbon nanotubes (CNT) are widely used in heterogeneous catalysis due to their chemical stability, low cost, and easily recovery of precious metals by means of combustion and other special properties in recent years C (Arrigo et al., 2012; Gao et al., 2018; Zhu et al., 2019). However, it is difficult to separate CNT supported catalysts after the liquid reaction due to its original powder form. Therefore, a macroscopic shaped CNT-based catalyst would facilitate the catalyst separating and handling which present a great potential either in the liquid phase and gas phase heterogeneous catalytic reactions (Liu et al., 2013, 2017; Ba et al., 2017; García-Bordejé et al., 2017).

In this work, monolithic CNT supported Pd catalyst is synthesized by one-pot process via combined palladium nitrate, CNT and alginate solution. During the synthesis process, the alginate played as biopolymer template to form alginate gel in the presence of CaCl₂ solution with a homogeneous size and macroscopic shape. The obtained monolithic Ca-Pd@CNT beads with different Ca promoter concentration were employed as catalyst for the hydrogenation of CAL to HCAL. The monolithic

structural carbon-based catalysts could be easily separated from the liquid reactant and thus facilitates the catalysts recycling. The structural and electronic properties of such monolithic Ca-Pd@CNT catalyst are analyzed by different characterization techniques to understand the structure-activity relationship in the presence of Ca promoter.

EXPERIMENTAL SECTION

Materials
The commercial multi-walled carbon nanotubes (CNT) were pre-treated by hydrochloric acid (6 mol/L) at room temperature for 12 h in order to remove residual metal impurities. CaCl₂, alginate and hydrochloric acid were purchased from Tianjin Kemiou Chemical Reagent Co., Ltd. (Tianjin, China). Pd (NO₃)₂ · 2H₂O was purchased from Alfa Aesar. All chemical agents were used as received without further purification.

Catalyst Preparation
Macroscopic shaped CNT beads (Liu et al., 2012; Ba et al., 2016):1 g of CNT was dispersed in 50 mL distilled water and treated by ultrasonic (400 W) for 60 min at room temperature. Then the mixture was heated to 50°C and maintained at this temperature for 10 min before a certain amount of alginate (1 wt.% with respect to the H₂O) was slowly added to the above mixture. The suspension was kept stirring under vigorous speed (500 rpm) at 50°C for another 50 min in order to obtain a homogeneous mixture. To form the gel beads, the mixture was added dropwise into an aqueous CaCl₂ (3 wt.%) solution at room temperature. The gel beads were left into CaCl₂ aqueous overnight, and then the gel beads were separated and washed with distilled water to remove excess sodium and calcium ions. The gel beads were dried under vacuum overnight and calcined at 350°C under argon for 2 h with the ramp of 2°C/min.

Ca-Pd@CNT$_{HCl-x}$ (x = 0, 2, 4) catalysts: Macroscopic shaped catalysts with 1 wt.% Pd loadings was synthesized by an *in-situ* process which was similar with aforementioned preparation method shown in **Figure 1**. Typically, the Pd(NO₃)₂·2H₂O was added into the CNT-containing suspension accompanied with the alginate. The gel beads were dried under vacuum and then calcined at 350°C under argon for 2 h with the ramp of 2°C/min to obtain the Ca-Pd@CNT sample. The as-synthesized Ca-Pd@CNT sample was reduced under pure H₂ at 400°C for 2 h. Furthermore, to investigate the influence of Ca promoter on the catalytic performance, the Ca-Pd@CNT sample was treated in dilute hydrochloric acid (1 mol/L) at room temperature for 2 and 4 h, respectively. HCl washed Ca-Pd@CNT sample were denoted as Ca-Pd@CNT$_{HCl-2h}$ and Ca-Pd@CNT$_{HCl-4h}$, respectively.

Pd/AC, Pd/CNT and macroscopic shaped Ca-Pd/CNT catalyst: A certain amount of Pd(NO₃)₂ solution was added into the active carbon (AC), powdered CNT and as-prepared CNT beads by wetness impregnation method. The samples were also dried under vacuum and calcined at 350°C under argon for 2 h with the ramp of 2°C/min, and then reduced under pure H₂ at 400°C for 2 h before the CAL chemoselsctive hydrogenation reaction.
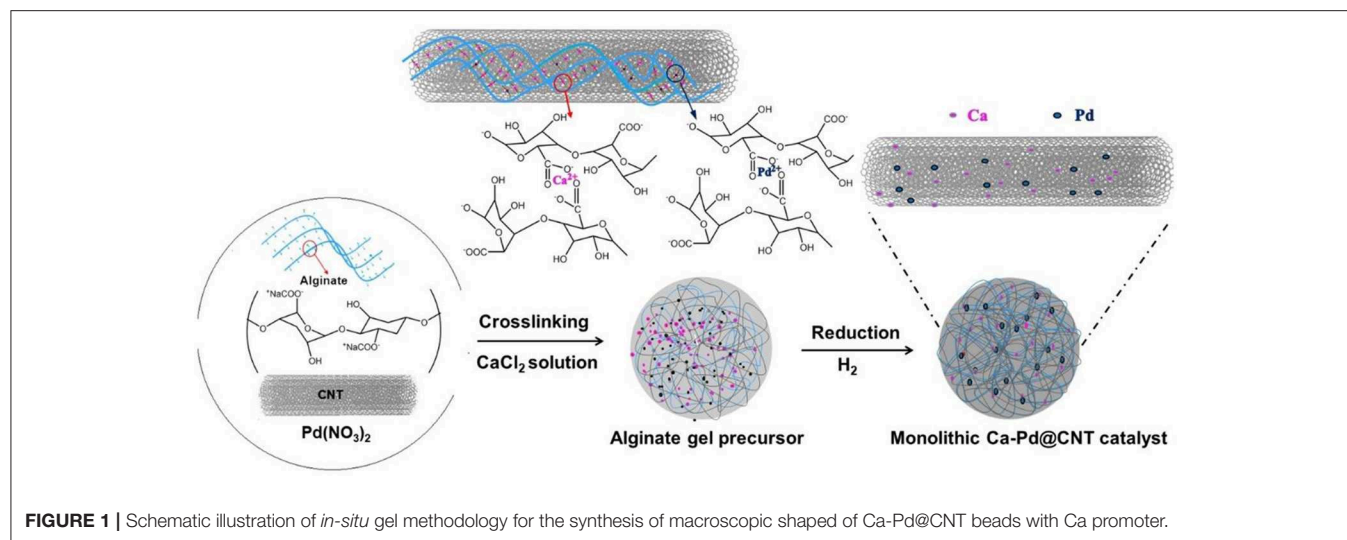
FIGURE 1 | Schematic illustration of *in-situ* gel methodology for the synthesis of macroscopic shaped of Ca-Pd@CNT beads with Ca promoter.

TABLE 1 | Specific surface area from N_2 adsorption-desorption isotherms, exactly Pd, Na, and Ca mass loading and catalytic performance in selective hydrogenation of CAL[a].

Catalyst	SAA (m^2/g)	Pd (wt.%)[b]	Ca (wt.%)[b]	Na (wt.%)[b]	d_{TEM} (nm)	CAL conversion (%)[b]	HCAL selectivity (%)
Pd/CNT	170	0.74	0	–	5.5	40.3	75.8
Ca-Pd@CNT	209	0.92	4.33	0.0308	4.7	63.8	86.5
Ca-Pd@CNT$_{HCl-2h}$	248	0.97	0.28	n.a.[c]	4.9	99.9	86.4
Ca-Pd@CNT$_{HCl-4h}$	303	0.93	0.06	–	4.9	92.1	86.5

[a] Reaction conditions: 10 bar H_2, 80°C, 30 mg of catalyst, 5 ml 0.45 mol/L reaction mixture, dioxane as solvent, o-xylene as internal standard, reaction time: 30 min.
[b] The actual mass loading of Pd and Ca (wt.%) on the various Ca-Pd@CNT catalysts were determined by ICP-OES.
[c] Not available.

Characterization

The morphology and compositions measurements were performed using a scanning electron microscopy (SEM) instrument (JSM-7800F, Japan), elemental mapping was operated on JSM-7800F with probe corrector at 15 kV. The textural properties of the samples were analyzed by N_2 adsorption-desorption measurements using a Micromeritics ASAP 2020 plus sorptometer operated at −196°C. The samples were degassed under vacuum at 180°C for 6 h before the analysis in order to desorb moisture and adsorbed volatile species on the sample surface. The specific surface area was calculated according to Brunauer-Emmett-Teller (BET) method. Pore volume and average pore diameter were determined from using desorption branch by Barret-Joyner-Halenda (BJH) method. Inductively coupled plasma optical emission spectrometer (ICP-OES) was used to measure Pd and Ca element concentration by an IRIS Intrepid II XSP instrument. The particle size was obtained through using Transmission electron microscopy (TEM) technology which was performed on Titan Themis ETEM G3 (Thermofisher) with image corrector operating at 300 kV. High angle annular dark filed scanning TEM (HAADF-STEM)

and elemental mapping were operated on Hitachi HF5000 with probe corrector at 200 kV. A small amount catalyst was crushed and ultrasonicated in ethanol, and then a drop was deposited onto a copper grid covered with a holey carbon membrane for analysis. X-ray photoelectron on spectroscopy (XPS) were recorded on a Thermofisher ESCALAB 250Xi spectrometer equipped with monochromatic Al KC (hυ = 1486.6 eV, 15 kV, 10.8 mA). The binding energies were calibrated by carbon deposit C1s with E_b = 284.6 eV.

Catalytic Reaction

The liquid phase hydrogenation of cinnamaldehyde was performed in an autoclave reactor with pressure control system. The reaction process as follows: cinnamaldehyde was diluted in 1,4-dioxane to obtain a 0.45 mol/L reaction solution, and o-xylene was used as internal standard. Typically, 30 mg of catalyst was added into 5 mL reaction solution. The autoclave was then purged with hydrogen flow with four times to replace the air inside the autoclave and maintained the total pressure at 1 MPa at room temperature. Then, the autoclave was heated to 80°C in a water bath with a magnetic stirrer at a fixed rate (c.a. 800 rpm) to carry out the hydrogenation reaction. After the reaction, the reaction mixture was analyzed using gas chromatograph (GC-FID) equipped with an HP-5 column.

The HCAL selectivity was calculated according to the following equation:

$$HCAL_{Selectivity}(\%) = \frac{\text{Moles of HCAL produced at reaction time}}{\text{Moles of CAL at converted at reaction time}} \times 100\% \quad (1)$$

RESULTS AND DISCUSSION

The macroscopic shaped Ca-Pd@CNT catalyst was synthesized by an ionic induced crosslinking method. A series of
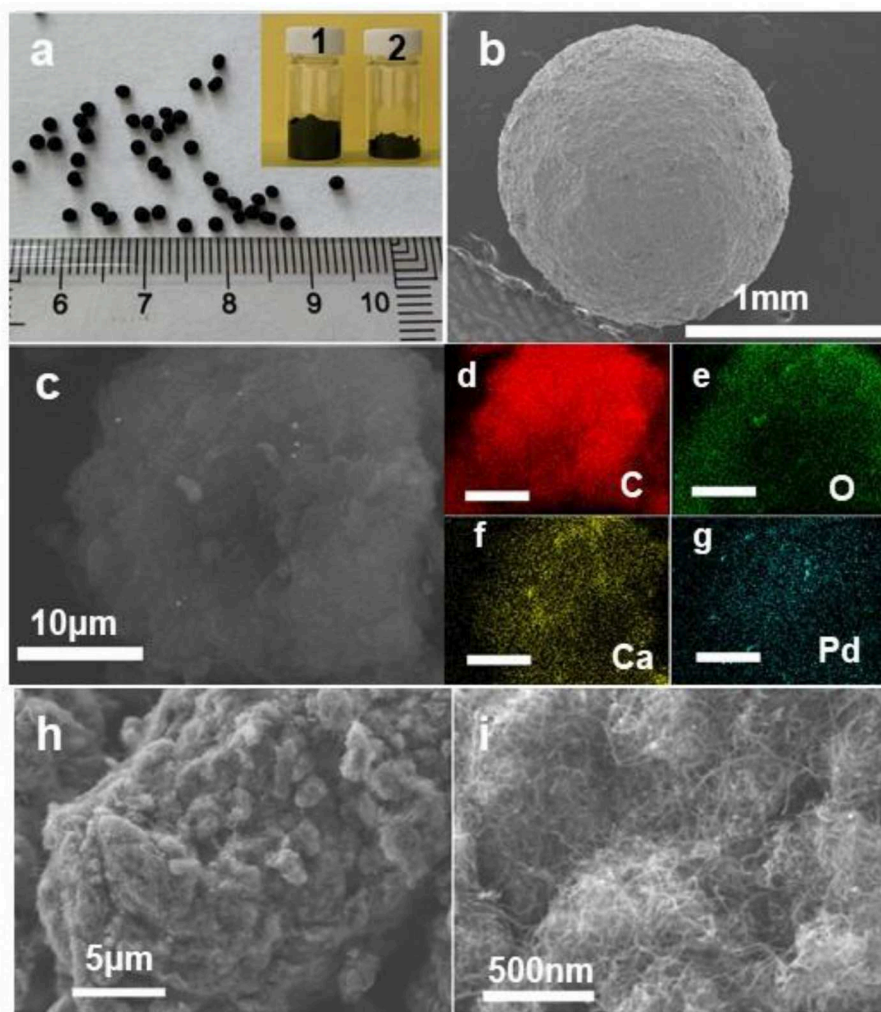
FIGURE 2 | (a) Optical photos showing macroscopic shaped Ca-Pd@CNT catalyst. The inset image presents the volume of hybrid catalyst (1) and the compared initial CNT sample (2). **(b)** Low magnification SEM micrograph showing the gross morphology of the sphere structured catalyst. **(c–g)** SEM image and elemental mapping of Ca-Pd@CNT catalyst. **(h,i)** SEM images of Ca-Pd@CNT catalysts show the opened structure of as-synthesized beads.

Ca-Pd@CNT beads catalysts with controlled macroscopic shaping was prepared with around 0.9 wt.% Pd loading which was confirmed through ICP-OES analysis (**Table 1**). As shown in **Figure 2**, the uniform spherical beads with homogeneous diameter around 1.5 mm could be formed successfully through the *in-situ* gel process. Compared to the initial CNT powder, the apparent volume of the shaped catalyst is smaller due to the shrinkage during the drying process (the inset digital photo of **Figure 2a**). The energy-dispersive X-ray (EDX) elemental mapping images of Ca-Pd@CNT beads (**Figures 2c–g**) showed that the Pd and Ca are uniformly dispersed on the Ca-Pd@CNT beads, and only few of them are aggregated in the macroscale. The element composition Ca-Pd@CNT beads derived from EDS spectra is 0.45 at% (Ca) and 0.09 at% (Pd) in atomic percentage, which is a little lower compared to the actual mass loading from the ICP-OES results (vide infra). The medium and high-resolution SEM images clearly show that CNT in the composites

entangled highly to form a large porosity dense network and the microscopic filamentous structure of CNT can be seen at high magnification. The above results indicated that highly dispersed particle could be obtained on the surface of CNT with a special macroscale structure through a simple preparation method.

TEM image of as-synthesized Ca-Pd@CNT beads reveals that the Pd NPs anchored on the surface of CNT with relatively homogeneous size (**Figure 3a**). The particle size distribution of Ca-Pd@CNT beads is centered at around 4.7 nm, while the comparative sample, Pd NPs supported on powdered CNT (Pd/CNT), displays an average particle size of 5.5 nm with a broaden size distribution (**Figure 3**). Such relative homogeneous Pd particle size on the Ca-Pd@CNT beads could be directly attribute to the strong interaction between the metal NPs with Ca species as well as the graphitic layers of support surface.

The chemoselective hydrogenation of cinnamaldehyde (CAL) to produce hydrocinnamaldehyde (HCAL) is selected as a probe
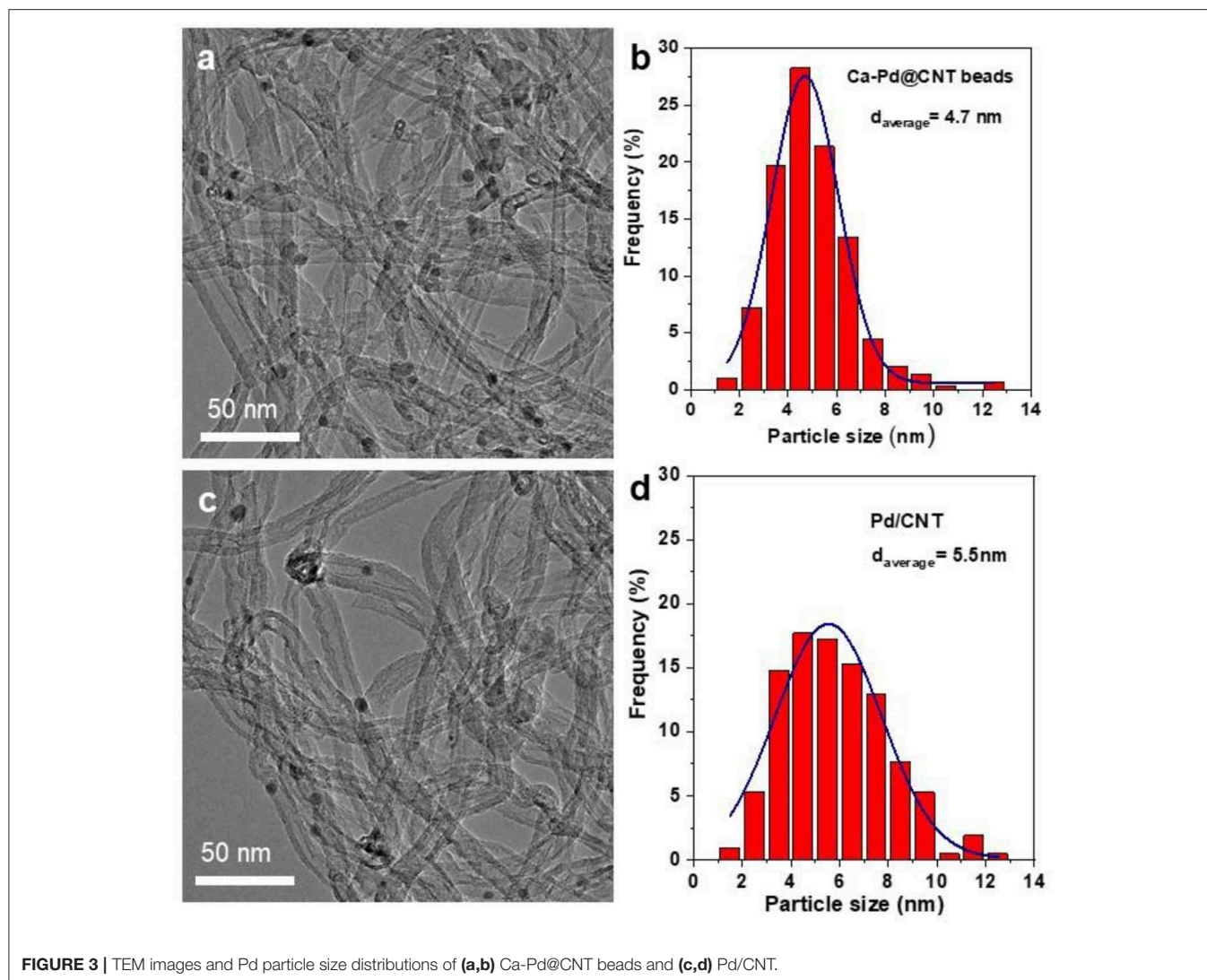
FIGURE 3 | TEM images and Pd particle size distributions of **(a,b)** Ca-Pd@CNT beads and **(c,d)** Pd/CNT.
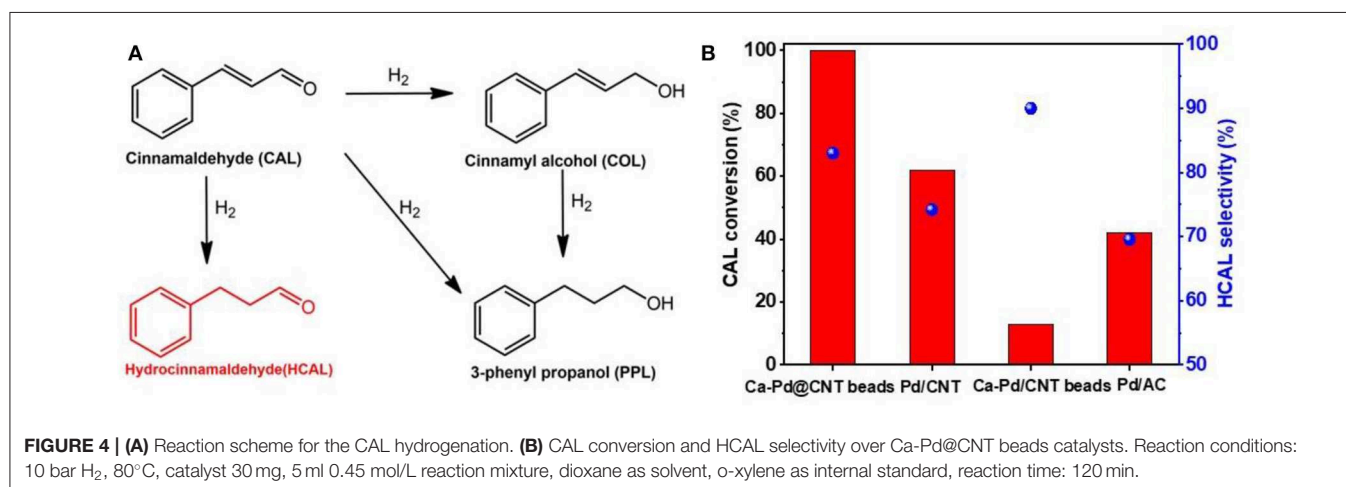

FIGURE 4 | (A) Reaction scheme for the CAL hydrogenation. **(B)** CAL conversion and HCAL selectivity over Ca-Pd@CNT beads catalysts. Reaction conditions: 10 bar H_2, 80°C, catalyst 30 mg, 5 ml 0.45 mol/L reaction mixture, dioxane as solvent, o-xylene as internal standard, reaction time: 120 min.

reaction to investigate the structure-activity of the as-synthesized Ca-Pd@CNT beads catalysts (**Figure 4A**). For comparison, Pd/CNT beads, Pd/AC and Pd/CNT were also synthesized by impregnation method by using as-synthesized CNT beads, AC, and original CNT as support, respectively (see experimental section). Specially, Pd/AC sample presents the largest Pd average
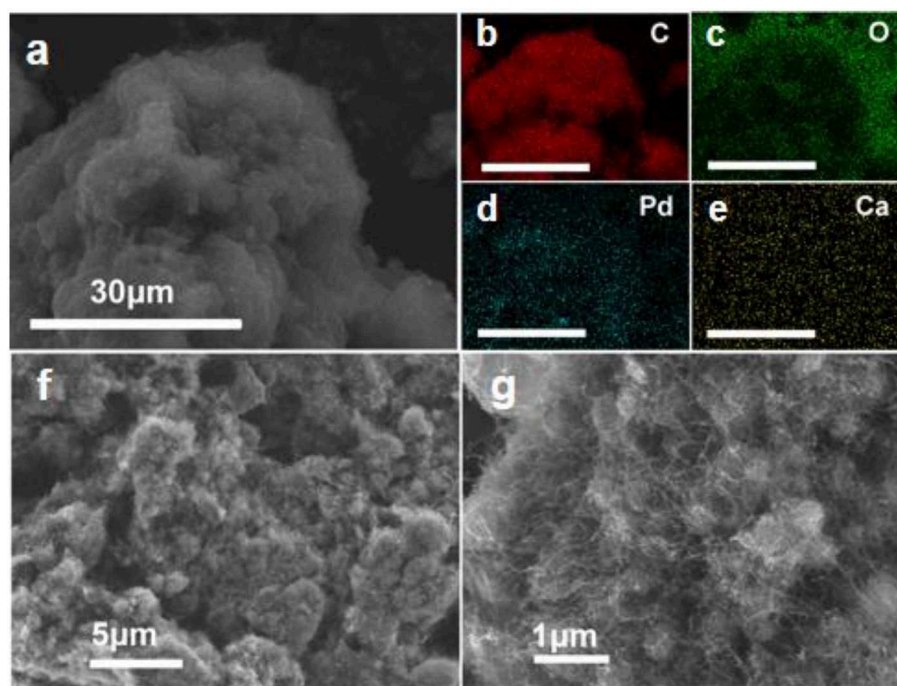
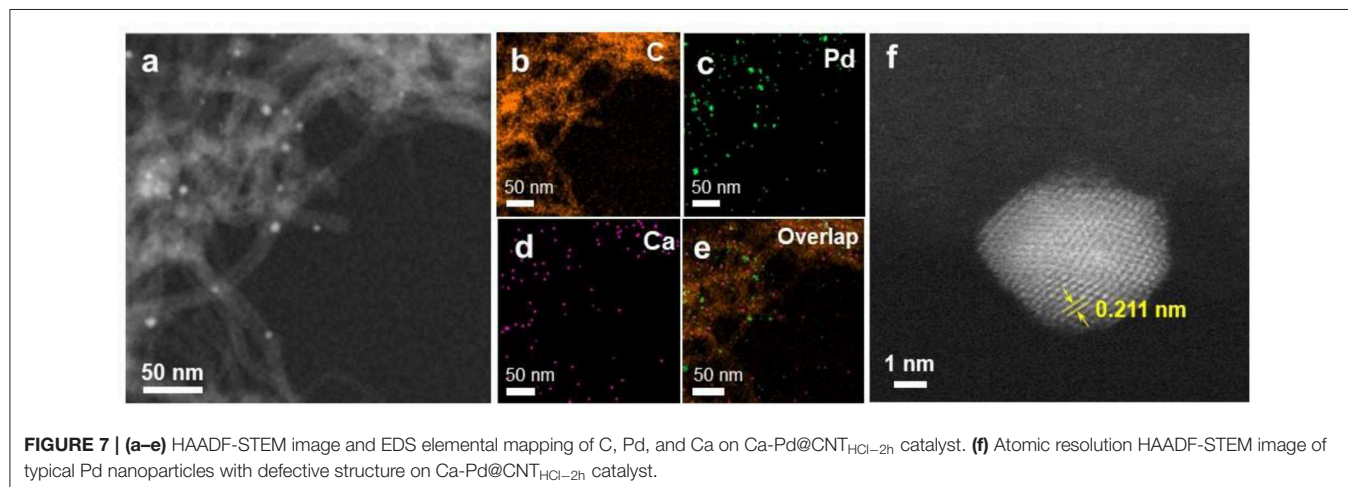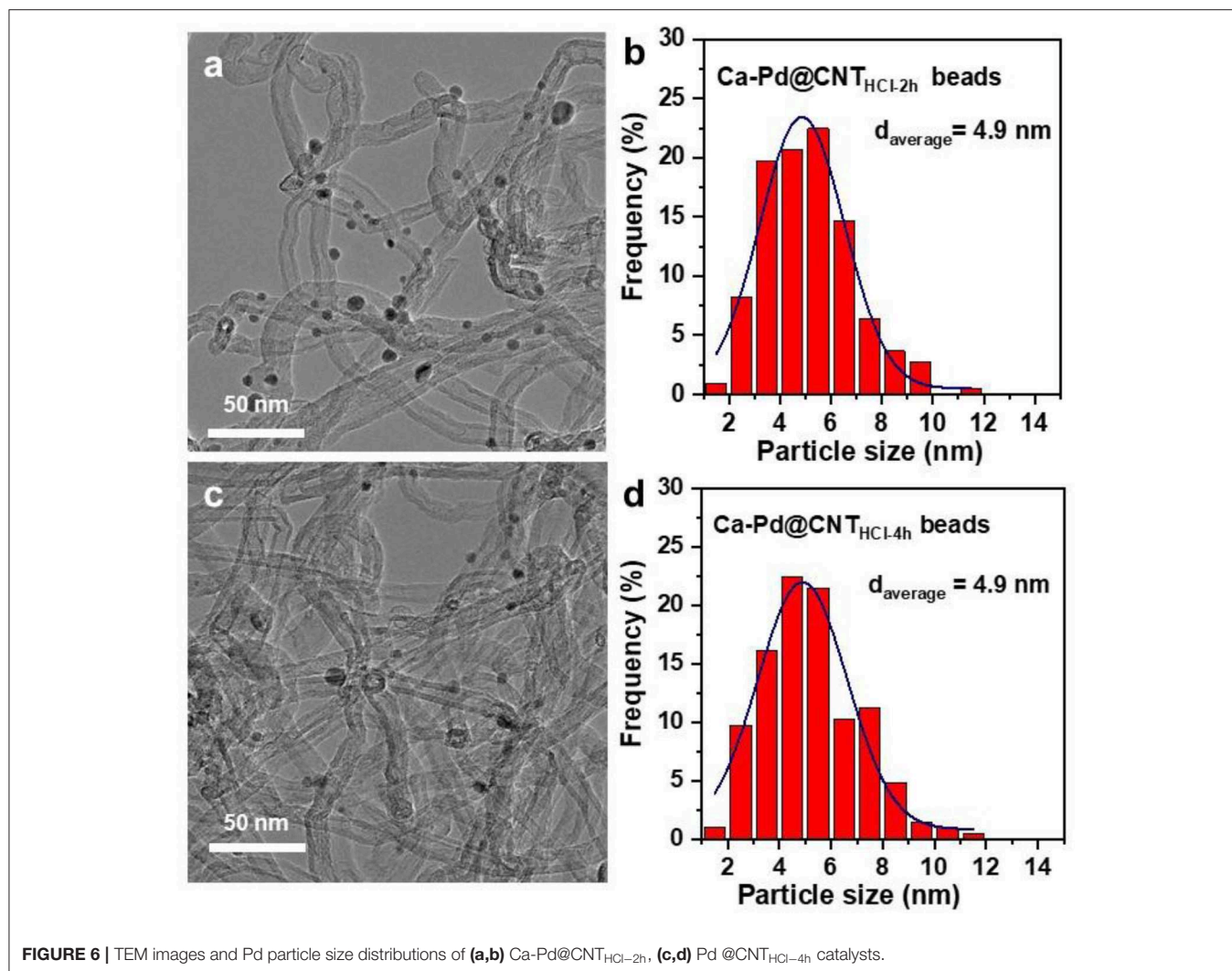**FIGURE 5 | (a–e)** EDS elemental mapping and **(f,g)** high resolution SEM images of Ca-Pd@CNT$_{HCl-2h}$ catalysts.

particle size at around 11.9 nm, which may be due to the weaken interaction between Pd NPs and active carbon (Jiang et al., 2016). The catalytic performances of CAL hydrogenation reaction and the corresponding HCAL selectivity over the various of supported Pd catalysts were displayed in **Figure 4B**. The selectivity of CAL to HCAL on Ca-Pd@CNT beads and Pd/CNT beads was relatively close (83.5 and 90.4%, respectively) under the same reaction conditions, whereas the CAL conversion on Ca-Pd@CNT beads (99.9%) was significantly higher than that of Pd/CNT beads (13.7%). It is obvious that the superior activity is obtained through the *in-situ* one-pot gel process. For Pd/AC and Pd/CNT catalysts, a lower HCAL selectivity was presented, 69.5 vs. 74.2%. Such lower selectively could be attributed to the bigger Pd particle size on Pd/AC catalyst (Xu et al., 2019). However, the possible reason for the relatively high HCAL selectivity compare to Pd/CNT catalyst could be that the presence of the additive Ca^{2+} ion during the catalyst preparation process (vide infra).

In order to identify the detailed role of the Ca^{2+} ion in this chemoselective hydrogenation process, the acid etching experiment was conducted over Ca-Pd@ CNT catalyst. To leach the different amount of Ca^{2+} ion, the diluted hydrochloric acid (HCl) with 1.0 mol/L is used and the etching time is fixed at 2 and 4 h, respectively. As shown in **Table 1**, the Ca mass concentration is amount to 4.33, 0.28, and 0.06 wt.% for Ca-Pd@CNT, Ca-Pd@CNT$_{HCl-2h}$, and Ca-Pd@CNT$_{HCl-4h}$, respectively, from the ICP-OES analysis. It is worth noting that the Pd mass weight is maintained at the similar value, c.a. 0.9 wt.% (**Table 1**), after acid etching. It means that the residual of Ca could be removed by the diluted HCl solution. The high-resolution SEM images and EDS

element mapping of Ca-Pd@CNT$_{HCl-2h}$ beads (**Figure 5**) show the morphology of the sample have not been destroyed during the acid treatment and the relative low Ca concentration is appeared by EDS elemental mapping.

The particle size distribution of Ca-Pd@CNT beads with acid etching for 2 and 4 h was shown in **Figure 6**. As expected, the Ca-Pd@CNT$_{HCl-2h}$ and Ca-Pd@CNT$_{HCl-4h}$ had similar particle sizes distribution and particle shapes compared to that of untreated Ca-Pd@CNT beads (**Figure 6**), indicating that acid treatment has no significant influence on the Pd microstructure. The typical Ca-Pd@CNT$_{HCl-2h}$ catalyst was further performed by atomic resolution STEM-HAADF for the microstructure analysis of calcium promoted Pd NPs (**Figure 7**). The EDS element mappings of Ca-Pd@CNT$_{HCl-2h}$ catalyst reveal that the Ca species are anchored on the surface of CNT and interacted with Pd NPs. The lattice of Pd nanoparticle 0.211 nm, which is related to the (111) facet of Pd (**Figure 7f**). It is suggested that that the Ca does not enter the lattice of Pd nanoparticles.

The Ca-Pd@CNT$_{HCl-2h}$ and Ca-Pd@CNT beads$_{HCl-4h}$ catalyst are reduced at 200°C under H_2 flow for CAL hydrogenation reaction. Compared to initial Ca-Pd@CNT catalyst, the CAL conversion of Ca-Pd@CNT$_{HCl-2h}$ increases significantly from 63.8% reach to 99.9%, and the HCAL selectivity remains approximately (c.a. 86.5%). It can be clearly seen that a lower concentration of calcium ion could be beneficial for the enhancement of catalytic activity. When the content of Ca^{2+} further declined to 0.06 wt.%, the CAL conversion of Ca-Pd@CNT$_{HCl-4h}$ is decreased to 92.1% with the similar HCAL selectivity 86.5%, which still presents superior catalytic activities compare to the Pd/CNT beads, Pd/CNT and Pd/AC catalysts. In

FIGURE 6 | TEM images and Pd particle size distributions of **(a,b)** Ca-Pd@CNT$_{HCl-2h}$, **(c,d)** Pd @CNT$_{HCl-4h}$ catalysts.

FIGURE 7 | (a–e) HAADF-STEM image and EDS elemental mapping of C, Pd, and Ca on Ca-Pd@CNT$_{HCl-2h}$ catalyst. **(f)** Atomic resolution HAADF-STEM image of typical Pd nanoparticles with defective structure on Ca-Pd@CNT$_{HCl-2h}$ catalyst.

addition, residual sodium could also plays the promotion role for noble metal nanoparticles in the hydrogenation reactions (King and Kelly, 2002; Kosydar et al., 2011; Long et al., 2019), where the sodium was also introduced during the synthesis process by

using alginate as gel source. However, the Na concentration of the initial Ca-Pd@CNT remained extremely low, i.e., 0.0308 wt.%, and cannot be accurately detected by ICP-OES technique for the further acid treated sample (Ca-Pd@CNTHCl-2h). It could be
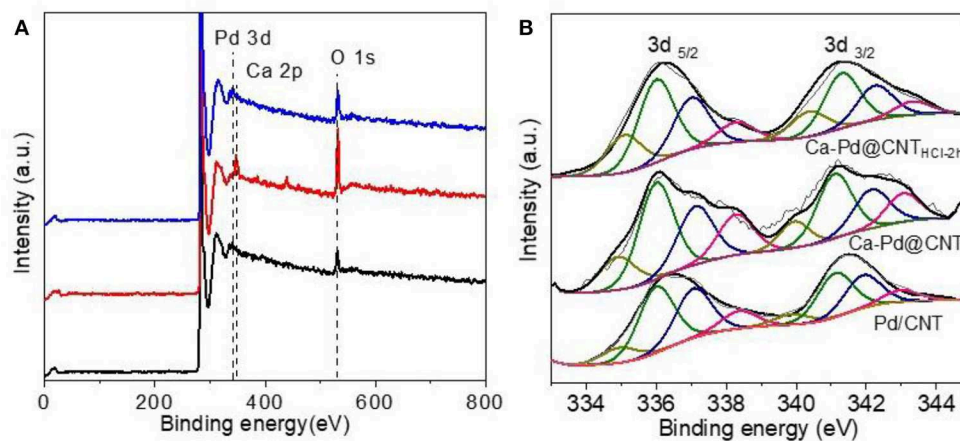
FIGURE 8 | (A) XPS survey spectra and high-resolution Pd 3d spectra of reduced Pd/CNT powder, Ca-Pd@CNT beads, and Ca-Pd@CNT$_{HCl-2h}$ beads. **(B)** The deconvoluted Pd 3d spectrum of reduced Pd/CNT powder, Ca-Pd@CNT beads, and Ca-Pd@CNTHCl-2h beads.

TABLE 2 | Elemental analysis of Pd $3d_{5/2}$ XPS spectra on monolithic Pd/CNT, Ca-Pd@CNT, and Ca-Pd@CNT$_{HCl-2h}$ catalysts.

Sample	Pd $3d_{5/2}$				
	Pd^0		$Pd^{\sigma+}$		$Pd^0/Pd^{\delta+}$
	BE/eV	at%	BE/eV	at%	
Pd/CNT	335.1	9.9	336.0	22.0	0.45
Ca-Pd@CNT	334.9	8.7	336.0	25.0	0.35
Ca-Pd@CNT$_{HCl-2h}$	334.9	6.2	336.0	26.7	0.23

revealed that Na could not affects the catalytic performance in this catalyst system. Thus, the results clearly demonstrate that in presence of Ca promoter can significantly increase the CAL hydrogenation activity, and the various Ca concentration could induce the different CAL hydrogenation ability. The extra Ca species covered on the surface of Pd NP could be etched during the moderate acid treatment process that result highly Pd active site exploration.

XPS survey spectra of Pd-decorated CNT are shown in **Figure 8A**. For the Pd/CNT sample, the XPS spectral show that distinct C 1s, O 1s, and Pd 3d peaks, and no other elements peaks are detected. The strong Pd 3d peaks are detected over the sample, suggesting that the formation of numerous Pd nanoparticles loaded on CNT carrier. In addition to the strong C 1s, O 1s, and Pd 3d peaks of Ca-Pd@CNT and Ca-Pd@CNT$_{HCl-2h}$ beads, which also has a strong Ca 2p and Ca 2s peak. The XPS analyses were conducted to reveal the electronic structure of the Pd species with or without the interaction of Ca ion (Rao et al., 2017). The XPS survey spectra of all samples show the expected elements (i.e., C, O. Pd) as well as the Ca that are derived from the cross-linking process for spherical Ca-Pd@CNT beads and Ca-Pd@CNT$_{HCl-2h}$ catalysts (**Figure 8A**). The deconvoluted Pd$_{3d}$ XPS spectra of Pd supported catalyst (**Figure 8B**) present two main peaks

at about 335.35 and 340.35 eV, corresponding to the doublet of Pd $3d_{5/2}$ and $3d_{3/2}$, respectively (Rao et al., 2017). The deconvolution of core level Pd$3d_{5/2}$ revealed the presence of predominant metallic phase (Pd^0, 335.1 eV), oxide state metal (Pd^{2+}, 337.0 eV) and a satellite peak (338.3 eV) (Pillo et al., 1997; Zhao et al., 2015; Arrigo et al., 2016). The oxide state Pd^{2+} was ascribed to the oxidation occurs on the surface of Pd NPs during the passivation process by diluted oxygen gas mixture (0.5 vol.% O$_2$ in helium). Furthermore, there was an apparent peak between Pd^0 and Pd^{2+} attribute to the electron transfer from Pd to the support, and then to produce the electron-depleted palladium species (Pd$^{\delta+}$) (Cárdenas-Lizana et al., 2013; Arrigo et al., 2016). As shown in **Table 2**, the lowest molar ratio of Pd^0/Pd$^{\delta+}$ is presented in Ca-Pd@CNT$_{HCl-2h}$ sample indicating that a certain amount of Ca promoter is in favor of forming Pd$^{\delta+}$ species which may in presence of electron transfer from Pd to Ca (Song et al., 2006), and thus accounts for the superior hydrogenation activity.

CONCLUSION

In conclusion, the *in-situ* gel process is employed successfully to prepare a controllable macroscopic shaped nanocarbon material containing Pd nanoparticle for chemoselective hydrogenation of CAL. The Ca promoter in the Ca-Pd@CNT beads is introduced by the interaction between Ca^{2+} ions and the hydroxyl and carboxyl groups of alginates during the cross-linking of alginate chains. As a result, the CAL hydrogenation activity is significantly enhanced in presence of Ca species through modifying the electron structure of Pd species. Compared to other prepared carbon-supported catalysts, the Ca-Pd@CNT$_{HCl-2h}$ with the moderate Ca loading displays the superior CAL hydrogenation activity as well as the HCAL selectivity which could be attributed to the lower Pd^0/Pd$^{\delta+}$ ratio in the catalyst. Besides, the controllable monolithic structure could endow the carbon-based catalyst easy handling during the reaction and recovery process

in the liquid-phase reaction. Moreover, such macroscopic process with *in-situ* introduced active metal species may also be applied in gas-phase reaction systems which could reduce the overall pressure drop across the packed bed comparing with the powered carbon-based catalysts.

DATA AVAILABILITY STATEMENT

The raw data supporting the conclusions of this manuscript will be made available by the authors, without undue reservation, to any qualified researcher.

AUTHOR CONTRIBUTIONS

YM and LF prepared the catalysts, conducted the characterization, reaction tests, and analyzed the data. JD prepared a part of catalysts. ZG conducted the HR-TEM analyses. CP-H contributed to thorough discussions on this work. YL designed the experiments and wrote the paper.

REFERENCES

Amorim, C., and Keane, M. A. (2008). Palladium supported on structured and nonstructured carbon: a consideration of Pd particle size and the nature of reactive hydrogen. *J. Colloid Interface Sci.* 322, 196–208. doi: 10.1016/j.jcis.2008.02.021

Arrigo, R., Schuster, M. E., Abate, S., Giorgianni, G., Centi, G., Perathoner, S., et al. (2016). Pd supported on carbon nitride boosts the direct hydrogen peroxide synthesis. *ACS Catal.* 6, 6959–6966. doi: 10.1021/acscatal.6b01889

Arrigo, R., Schuster, M. E., Abate, S., Wrabetz, S., Amakawa, K., Teschner, D., et al. (2014). Dynamics of palladium on nanocarbon in the direct synthesis of H_2O_2. *ChemSusChem* 7, 179–194. doi: 10.1002/cssc.201300616

Arrigo, R., Schuster, M. E., Wrabetz, S., Girgsdies, F., Tessonnier, J.-P., Centi, G., et al. (2012). New insights from microcalorimetry on the FeOx/CNT-based electrocatalysts active in the conversion of CO_2 to fuels. *ChemSusChem* 5, 577–586. doi: 10.1002/cssc.201100641

Auer, E., Freund, A., Pietsch, J., and Tacke, T. (1998). Carbons as supports for industrial precious metal catalysts. *Appl. Catal. A Gen.* 173, 259–271. doi: 10.1016/S0926-860X(98)00184-7

Ba, H., Duong-Viet, C., Liu, Y., Nhut, J.-M., Granger, P., Ledoux, M. J., et al. (2016). Nitrogen-doped carbon nanotube spheres as metal-free catalysts for the partial oxidation of H2S. *Comptes Rendus Chim.* 19, 1303–1309. doi: 10.1016/j.crci.2015.09.022

Ba, H., Luo, J., Liu, Y., Duong-Viet, C., Tuci, G., Giambastiani, G., et al. (2017). Macroscopically shaped monolith of nanodiamonds @ nitrogen-enriched mesoporous carbon decorated SiC as a superior metal-free catalyst for the styrene production. *Appl. Catal. B Environ.* 200, 343–350. doi: 10.1016/j.apcatb.2016.07.014

Balmes, O., Resta, A., Wermeille, D., Felici, R., Messing, M. E., Deppert, K., et al. (2012). Reversible formation of a PdC(x) phase in Pd nanoparticles upon CO and O_2 exposure. *Phys. Chem. Chem. Phys.* 14, 4796–4801. doi: 10.1039/c2cp22873d

Bhogeswararao, S., and Srinivas, D. (2012). Intramolecular selective hydrogenation of cinnamaldehyde over CeO_2–ZrO_2-supported Pt catalysts. *J. Catal.* 285, 31–40. doi: 10.1016/j.jcat.2011.09.006

Cárdenas-Lizana, F., Hao, Y., Crespo-Quesada, M., Yuranov, I., Wang, X., Keane, M. A., et al. (2013). selective gas phase hydrogenation of p-chloronitrobenzene over Pd catalysts: role of the support. *ACS Catal.* 3, 1386–1396. doi: 10.1021/cs4001943

Daly, H., Manyar, H. G., Morgan, R., Thompson, J. M., Delgado, J. J., Burch, R., et al. (2014). Use of short time-on-stream attenuated total internal reflection infrared spectroscopy to probe changes in adsorption geometry for determination of selectivity in the hydrogenation of citral. *ACS Catal.* 4, 2470–2478. doi: 10.1021/cs500185n

Durndell, L. J., Parlett, C. M., Hondow, N. S., Isaacs, M. A., Wilson, K., and Lee, A. F. (2015). Selectivity control in Pt-catalyzed cinnamaldehyde hydrogenation. *Sci. Rep.* 5:9425. doi: 10.1038/srep09425

Figueiredo, J. L. (2013). Functionalization of porous carbons for catalytic applications. *J. Mater. Chem. A* 1, 9351–9364. doi: 10.1039/c3ta10876g

Gallezot, P., and Richard, D. (1998). Selective hydrogenation of α,β-unsaturated aldehydes. *Catal. Rev.* 40, 81–126. doi: 10.1080/01614949808007106

Galvagno, S., Poltarzewski, Z., Donato, A., Neri, G., and Pietropaolo, R. (1986). Selective hydrogenation of alpha, beta-unsaturated aldehydes to give unsaturated alcohols over platinum germanium catalysts. *J. Chem. Soc. Chem. Commun.* 23, 1729–1731. doi: 10.1039/C39860001729

Gao, J., Jiang, Q., Liu, Y., Liu, W., Chu, W., and Su, D. S. (2018). Probing the enhanced catalytic activity of carbon nanotube supported Ni-LaOx hybrids for the CO_2 reduction reaction. *Nanoscale* 10, 14207–14219. doi: 10.1039/C8NR03882A

García-Bordejé, E., Liu, Y., Su, D. S., and Pham-Huu, C. (2017). Hierarchically structured reactors containing nanocarbons for intensification of chemical reactions. *J. Mater. Chem. A* 5, 22408–22441. doi: 10.1039/C7TA06826C

Garcia-Mota, M., Bridier, B., Perez-Ramirez, J., and Lopez, N. (2010). Interplay between carbon monoxide, hydrides, and carbides in selective alkyne hydrogenation on palladium. *J. Catal.* 273, 92–102. doi: 10.1016/j.jcat.2010.04.018

Hsu, C.-Y., Chiu, T.-C., Shih, M.-H., Tsai, W.-J., Chen, W.-Y., and Lin, C.-H. (2010). Effect of electron density of Pt catalysts supported on alkali titanate nanotubes in cinnamaldehyde hydrogenation. *J. Phys. Chem. C*, 114, 4502–4510. doi: 10.1021/jp9095198

Ide, M. S., Hao, B., Neurock, M., and Davis, R. J. (2012). Mechanistic insights on the hydrogenation of α,β-unsaturated ketones and aldehydes to unsaturated alcohols over metal catalysts. *ACS Catal.* 2, 671–683. doi: 10.1021/cs200567z

Jiang, F., Cai, J., Liu, B., Xu, Y., and Liu, X. (2016). Particle size effects in the selective hydrogenation of cinnamaldehyde over supported palladium catalysts. *RSC Adv.* 6, 75541–75551. doi: 10.1039/C6RA17000E

Kahsar, K. R., Schwartz, D. K., and Medlin, J. W. (2014). Control of metal catalyst selectivity through specific noncovalent molecular interactions. *J. Am. Chem. Soc.* 136, 520–526. doi: 10.1021/ja411973p

King, F., and Kelly, G. J. (2002). Combined solid base/hydrogenation catalysts for industrial condensation reactions. *Catal. Today* 73, 75–81. doi: 10.1016/S0920-5861(01)00520-X

Kosydar, R., Drelinkiewicz, A., Lalik, E., and Gurgul, J. (2011). The role of alkali modifiers (Li, Na, K, Cs) in activity of 2%Pd/Al_2O_3 catalysts for 2-ethyl-9,10-anthraquione hydrogenation. *Appl. Catal. A Gen.* 402, 121–131. doi: 10.1016/j.apcata.2011.05.036

Li, G. J., Li, T., Xu, Y. D., Wong, S.-T., and Guo, X.-X. (1997). Selective hydrogenation of cinnamaldehyde to cinnamyl alcohol on L-zeolite supported catalysts. *Stud. Surface Sci. Catal.* 105, 1203–1210. doi: 10.1016/S0167-2991(97)80758-6

Liu, Y., Ba, H., Nguyen, D.-L., Ersen, O., Romero, T., Zafeiratos, S., et al. (2013). Synthesis of porous carbon nanotubes foam composites with a high accessible surface area and tunable porosity. *J. Mater. Chem. A* 1, 9508–9516. doi: 10.1039/c3ta10695k

Liu, Y., Luo, J., Helleu, C., Behr, M., Ba, H., Romero, T., et al. (2017). Hierarchical porous carbon fibers/carbon nanofibers monolith from electrospinning/CVD processes as a high effective surface area support platform. *J. Mater. Chem. A* 5, 2151–2162. doi: 10.1039/C6TA09414G

Liu, Y., Nguyen, L. D., Truong-Huu, T., Liu, Y., Romero, T., Janowska, I., et al. (2012). Macroscopic shaping of carbon nanotubes with high specific surface area and full accessibility. *Mater. Lett.* 79, 128–131. doi: 10.1016/j.matlet.2012.03.107

Long, Y., Wang, Y., Wu, H., Xue, T., Wu, P., and Guan, Y. (2019). Doping Pd/SiO$_2$ with Na+: changing the reductive etherification of C=O to furan ring hydrogenation of furfural in ethanol. *RSC Adv.* 9, 25345–25350. doi: 10.1039/C9RA05281J

Mäki-Arvela, P., Hájek, J., Salmi, T., and Murzin, D. Y. (2005). Chemoselective hydrogenation of carbonyl compounds over heterogeneous catalysts. *Appl. Catal. A Gen.* 292, 1–49. doi: 10.1016/j.apcata.2005.05.045

Pillo, T., Zimmermann, R., Steiner, P., and Hufner, S. (1997). The electronic structure of PdO found by photoemission (UPS and XPS) and inverse photoemission (BIS). *J. Phys. Cond. Matter* 9, 3987–3999. doi: 10.1088/0953-8984/9/19/018

Rao, R. G., Blume, R., Hansen, T. W., Fuentes, E., Dreyer, K., Moldovan, S., et al. (2017). Interfacial charge distributions in carbon-supported palladium catalysts. *Nat. Commun.* 8:340. doi: 10.1038/s41467-017-00421-x

Salnikov, O. G., Kovtunov, K. V., Barskiy, D. A., Khudorozhkov, A. K., Inozemtseva, E. A., Prosvirin, I. P., et al. (2014). Evaluation of the mechanism of heterogeneous hydrogenation of α,β-unsaturated carbonyl compounds via pairwise hydrogen addition. *ACS Catal.* 4, 2022–2028. doi: 10.1021/cs500426a

Song, J.-R., Wen, L.-X., Shao, L., and Chen, J.-F. (2006). Preparation and characterization of novel Pd/SiO$_2$ and Ca–Pd/SiO$_2$ egg-shell catalysts with porous hollow silica. *Appl. Surf. Sci.* 253, 2678–2684. doi: 10.1016/j.apsusc.2006.05.035

Su, D. S., Perathoner, S., and Centi, G. (2013). Nanocarbons for the development of advanced catalysts. *Chem. Rev.* 113, 5782–5816. doi: 10.1021/cr300367d

Tian, Z., Liu, C., Li, Q., Hou, J., Li, Y., and Ai, S. (2015). Nitrogen- and oxygen-functionalized carbon nanotubes supported Pt-based catalyst for the selective hydrogenation of cinnamaldehyde. *Appl. Catal. A Gen.* 506, 134–142. doi: 10.1016/j.apcata.2015.08.023

Toebes, M. (2004). Support effects in the hydrogenation of cinnamaldehyde over carbon nanofiber-supported platinum catalysts: characterization and catalysis. *J. Catal.* 226, 215–225. doi: 10.1016/j.jcat.2004.05.026

Tsang, S. C., Cailuo, N., Oduro, W., Kong, A. T. S., Clifton, L., Yu, K. M. K., et al. (2008). Engineering preformed cobalt-doped platinum nanocatalysts for ultraselective hydrogenation. *Acs Nano* 2, 2547–2553. doi: 10.1021/nn800400u

Vu, H., Goncalves, F., Philippe, R., Lamouroux, E., Corrias, M., Kihn, Y., et al. (2006). Bimetallic catalysis on carbon nanotubes for the selective hydrogenation of cinnamaldehyde. *J. Catal.* 240, 18–22. doi: 10.1016/j.jcat.2006.03.003

Wei, H., Ren, Y., Wang, A., Liu, X., Liu, X., Zhang, L., et al. (2017). Remarkable effect of alkalis on the chemoselective hydrogenation of functionalized nitroarenes over high-loading Pt/FeO x catalysts. *Chem. Sci.* 8, 5126–5131. doi: 10.1039/C7SC00568G

Wu, B., Huang, H., Yang, J., Zheng, N., and Fu, G. (2012). Selective hydrogenation of alpha,beta-unsaturated aldehydes catalyzed by amine-capped platinum-cobalt nanocrystals. *Angew. Chem. Int. Ed Engl.* 51, 3440–3443. doi: 10.1002/anie.201108593

Xu, Z., Duong-Viet, C., Liu, Y., Baaziz, W., Li, B., Nguyen-Dinh, L., et al. (2019). Macroscopic graphite felt containing palladium catalyst for liquid-phase hydrogenation of cinnamaldehyde. *Appl. Catal. B Environ.* 244, 128–139. doi: 10.1016/j.apcatb.2018.11.041

Yang, X., Su, X., Chen, X., Duan, H., Liang, B., Liu, Q., et al. (2017). Promotion effects of potassium on the activity and selectivity of Pt/zeolite catalysts for reverse water gas shift reaction. *Appl. Catal. B Environ.* 216, 95–105. doi: 10.1016/j.apcatb.2017.05.067

Zhao, Z., Huang, X., Li, M., Wang, G., Lee, C., Zhu, E., et al. (2015). Synthesis of stable shape-controlled catalytically active beta-palladium hydride. *J. Am. Chem. Soc.* 137, 15672–15675. doi: 10.1021/jacs.5b11543

Zhu, J., Dou, M., Lu, M., Xiang, X., Ding, X., Liu, W., et al. (2019). Thermo-responsive polymer grafted carbon nanotubes as the catalyst support for selective hydrogenation of cinnamaldehyde: effects of surface chemistry on catalytic performance. *Appl. Catal. A Gen.* 575, 11–19. doi: 10.1016/j.apcata.2019.02.009